Supporting Information for:

Cell Penetration Profiling Using the Chloroalkane Penetration Assay

Leila Peraro[1], Kirsten L. Deprey[1], Matthew K. Moser,[1] Zhongju Zou[2,3], Haydn L. Ball,[2] Beth Levine[2-4], Joshua A. Kritzer[1,*]

[1]Department of Chemistry, Tufts University, Medford, MA 02155, [2]Center for Autophagy Research, Department of Internal Medicine, University of Texas Southwestern Medical Center, Dallas, TX 75230, [3]Howard Hughes Medical Institute, University of Texas Southwestern Medical Center, Dallas, TX 75230, [4]Department of Microbiology, University of Texas Southwestern Medical Center, Dallas, TX 75230. *Corresponding author: joshua.kritzer@tufts.edu

Supporting Figures, Tables

SI Table 1. Peptide names, sequences and observed masses.

Peptide	Sequence	Staple	Calculated $[M+H]^+$	Observed $[M+H]^+$
ct-W	ct-W	-	509.0	509.6
ct-Tat	ct-YGRKKRRQRRR	-	1879.7	1881.3
ct-Arg9	ct-RRRRRRRRRW	-	1914.8	1915.2
ct-Antp	ct-RQIKIWFQNRRMKWKK	-	2551.6	2552.5
ct-ZF5.3	ct-WYSCNVCGKAFVLSRHLNRHLRVHRRAT	-	3685.8	3688.4
ct-DP1	[FΦRRRRE]K(ct)W	sidechain-to-N-term lactam	1717.5	1719.2
ct-SAHB	ct-IWIAQELR(S_5)IGD(S_5)FNAYYARR	hydrocarbon	2910.9	2912.8
ct-PEG_2-W	ct-PEG_2-W	-	654.2	653.8
ct-PEG_2-Tat	ct-PEG_2-YGRKKRRQRRR	-	2009.8	2009.5
ct-PEG_2-Arg9	ct-PEG_2-RRRRRRRRRW	-	2059.9	2058.9
ct-PEG_2-Antp	ct-PEG_2-RQIKIWFQNRRMKWKK	-	2696.7	2698.6
ct-PEG_2-ZF5.3	ct-PEG_2-WYSCNVCGKAFVLSRHLNRHLRVHRRAT	-	3830.9	3831.2
ct-PEG_2-DP1	[FΦRRRRQ]K(PEG_2-ct)W	sidechain-to-N-term lactam	1862.7	1862.8
ct-DD5o-pa	ct-VcNACFHIWHK(pa)	*o*-xylene	1845.6	1846.3
pa-DD5o-ct	pa-VcNACFHIWHK(ct)	*o*-xylene	1845.6	1847.1
ct-DD5o	ct-VcNAcFHIWH	*o*-xylene	1636.4	1637.4
ct-PEG_2-DD5o	ct-PEG_2-VcNAcFHIWH	*o*-xylene	1781.6	1780.4
ct-PEG_3-DD5o	ct-PEG_3-VcNAcFHIWH	*o*-xylene	1825.6	1825.0
ct-PEG_4-DD5o	ct-PEG_4-VcNAcFHIWH	*o*-xylene	1869.7	1869.2
ct-hex-DD5o	ct-hex-VcNAcFHIWH	*o*-xylene	1749.6	1749.1
ct-DD5o-V1A	ct-AcNAcFHIWH	*o*-xylene	1608.3	1609.1
ct-DD5o-N3A	ct-VcAAcFHIWH	*o*-xylene	1593.4	1592.9
ct-DD5o-F6A	ct-VcNAcAHIWH	*o*-xylene	1560.3	1563.6
ct-DD5o-H7A	ct-VcNAcFAIWH	*o*-xylene	1570.3	1571.0
ct-DD5o-I8A	ct-VcNAcFHAWH	*o*-xylene	1594.3	1593.6
ct-DD5o-W9A	ct-VcNAcFHIAH	*o*-xylene	1521.3	1521.9
ct-DD5o-H10A	ct-VcNAcFHIWA	*o*-xylene	1570.3	1570.4
ct-PEG_2-DD5o-V1A	ct-PEG_2-AcNAcFHIWH	*o*-xylene	1753.5	1751.8
ct-PEG_2-DD5o-N3A	ct-PEG_2-VcAAcFHIWH	*o*-xylene	1738.5	1737.2
ct-PEG_2-DD5o-F6A	ct-PEG_2-VcNAcAHIWH	*o*-xylene	1705.5	1706.6
ct-PEG_2-DD5o-H7A	ct-PEG_2-VcNAcFAIWH	*o*-xylene	1715.5	1715.1
ct-PEG_2-DD5o-I8A	ct-PEG_2-VcNAcFHAWH	*o*-xylene	1739.5	1739.8
ct-PEG_2-DD5o-W9A	ct-PEG_2-VcNAcFHIAH	*o*-xylene	1666.4	1665.1

ct-PEG_2-DD5o-H10A	ct-PEG_2-VcNAcFHIWA	*o*-xylene	1715.5	1716.0
ct-V1Aep	ct-(Aep)cNAcFHIWH	*o*-xylene	1664.4	1664.9
ct-Tat-11mer	ct-YGRKKRRQRRRGGVWNATFHIWHD	-	3386.3	3387.2
ct-Tat-11scr	ct-YGRKKRRQRRRGGWNHADHTFVWI	-	3386.3	3387.2
ct-11mer-Tat	ct-VWNATFHIWHDGGYGRKKRRQRRR	-	3386.3	3387.2
ct-11mer-Tat-M1	ct-VWNATAHIWHDGGYGRKKRRQRRR	-	3310.2	3311.1
ct-11mer-Tat-M2	ct-VWNATFHAWHDGGYGRKKRRQRRR	-	3344.3	3345.2
ct-11mer-Tat-M3	ct-VWNATAHAWHDGGYGRKKRRQRRR	-	3268.2	3269.1
ct-11mer-Tat-M4	ct-VANATFHIWHDGGYGRKKRRQRRR	-	3271.2	3272.1
ct-Arg9-11mer	ct-RRRRRRRRRGGVWNATFHIWHD	-	3250.2	3251.0
ct-Arg9-11mer-M1	ct-RRRRRRRRRGGVWNATAHIWHD	-	3174.1	3175.0
ct-Arg9-11mer-M2	ct-RRRRRRRRRGGVWNATFHAWHD	-	3208.1	3209.0
ct-Arg9-11mer-M3	ct-RRRRRRRRRGGVWNATAHAWHD	-	3132.0	3133.0
ct-Arg9-11mer-M4	ct-RRRRRRRRRGGVANATFHIWHD	-	3135.1	3136.0
ct-PEG_4-biotin	ct-PEG_4-biotin	-	697.3	697.5

ct = chloroalkane tag (see Figure S1 for structure), c = D-cysteine, Φ = 2-naphthylalanine, S_5 = S-pentenylalanine, pa = pentynoic acid, [ ] = N-terminus to E-sidechain cyclization, Aep = 2-amino-3-ethyl-pentanoic acid

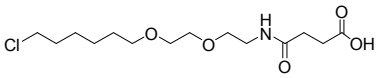

ct-COOH

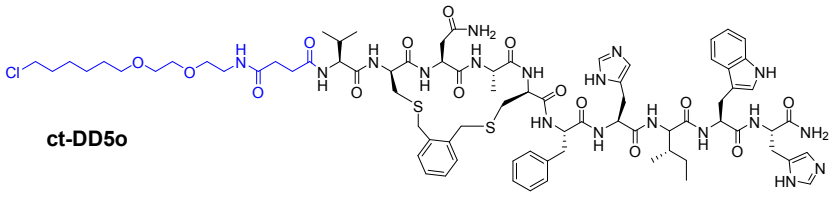

ct-DD5o

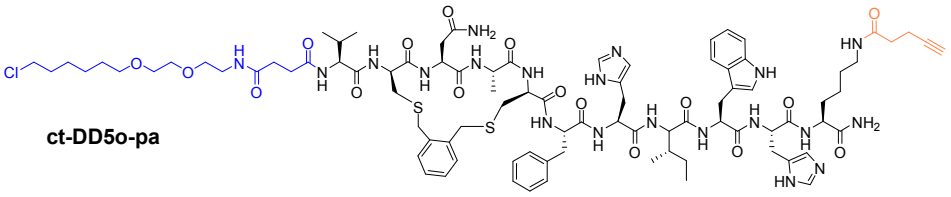

ct-DD5o-pa

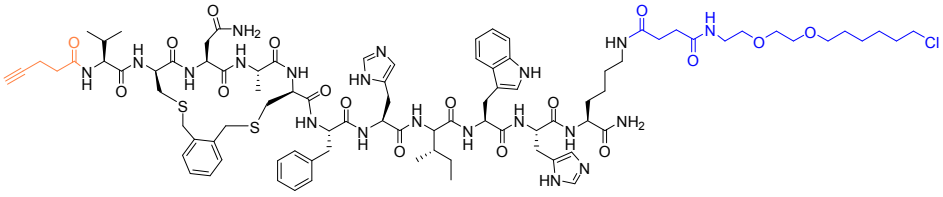

pa-DD5o-ct

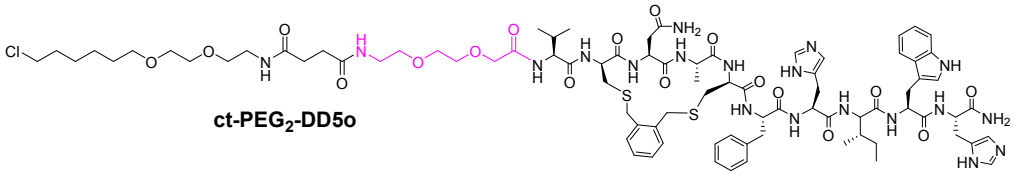

ct-PEG$_2$-DD5o

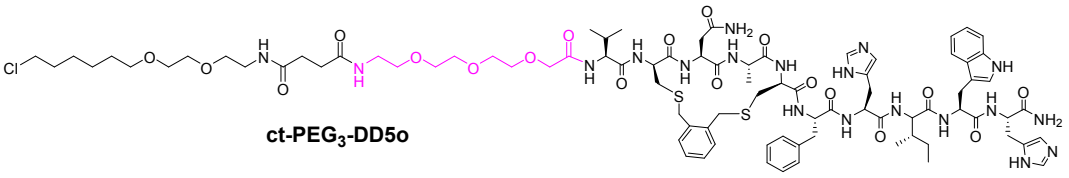

ct-PEG$_3$-DD5o

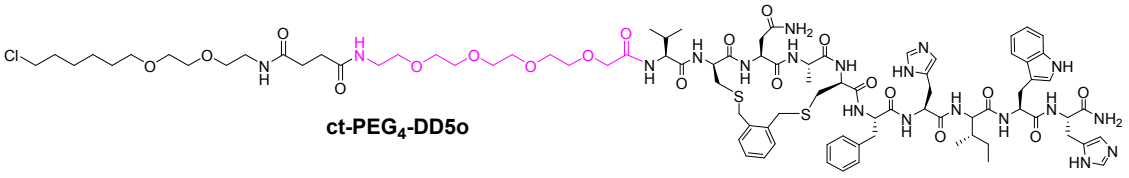

ct-PEG$_4$-DD5o

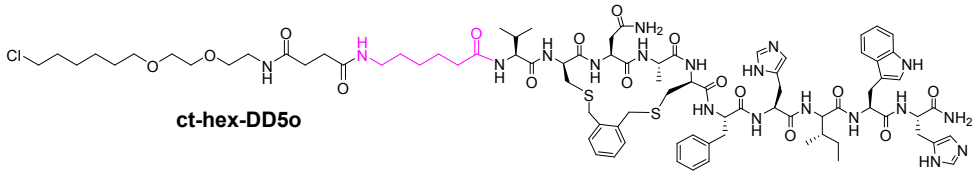

ct-hex-DD5o

SI Figure 1. Chemical structures of selected compounds (continued on next page).

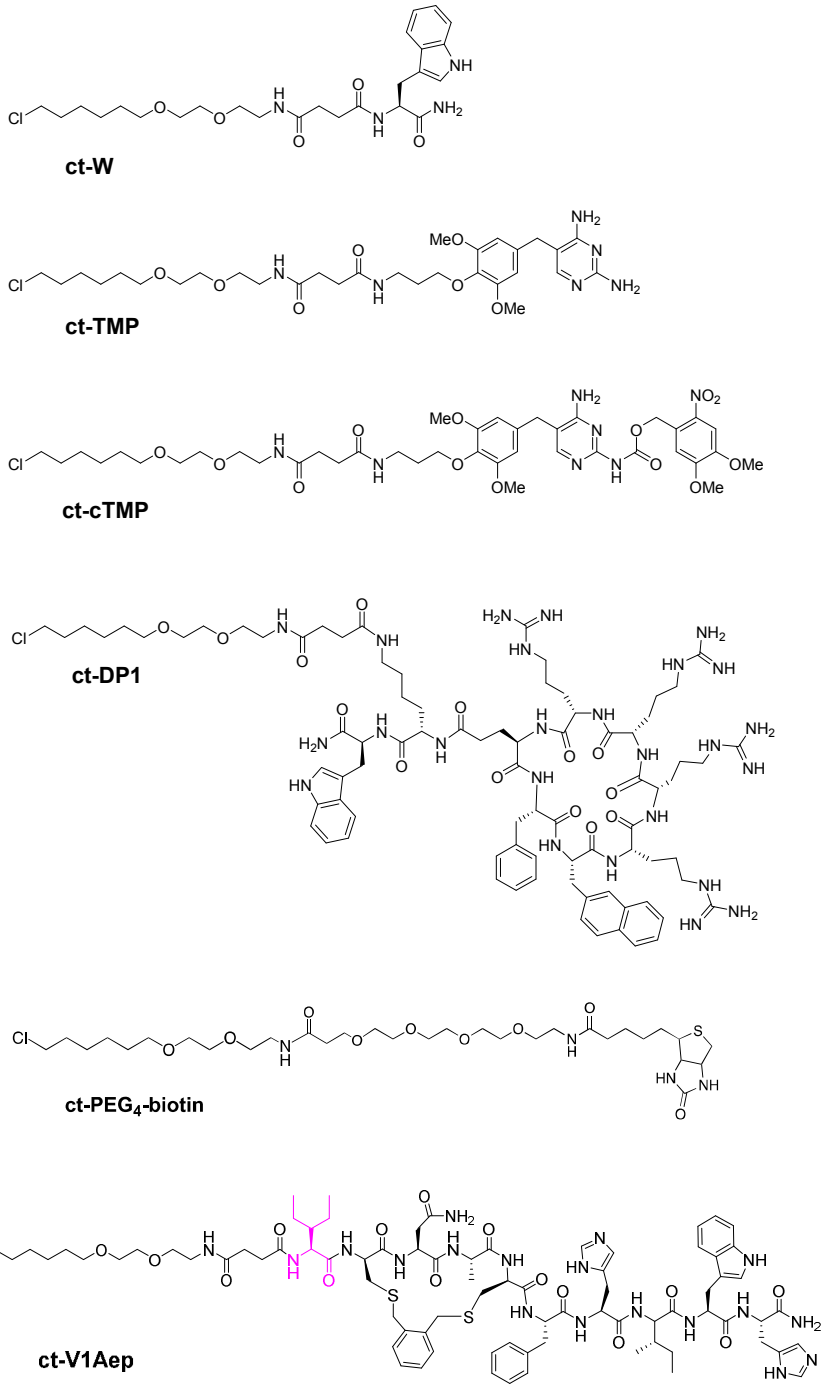

SI Figure 1 (continued). Chemical structures of selected compounds.

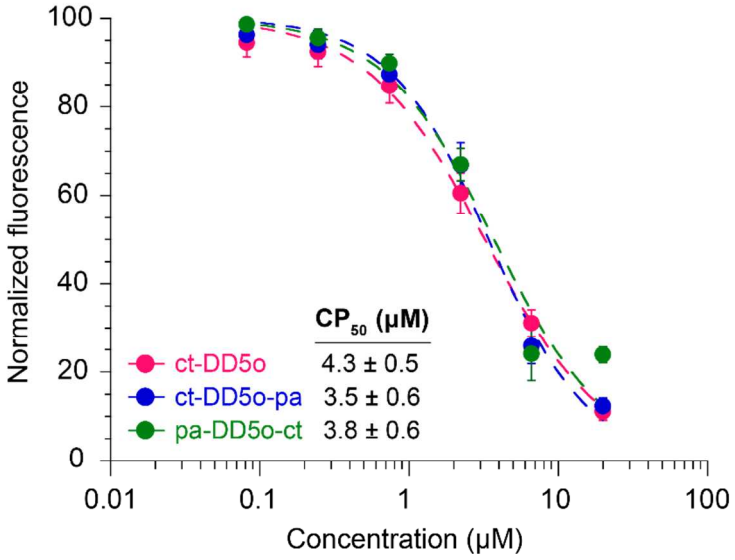

SI Figure 2. Varying location of chloroalkane tag has very little effect on CAPA results for DD5o. Dose-dependent CAPA results for ct-DD5o, ct-DD5o-pa, and pa-DD5o-ct. ct-DD5o-pa differs from ct-DD5o in that it has an additional lysine on the C-terminus, and the lysine is acylated with 4-pentynoic acid. pa-DD5o-ct is isomeric with ct-DD5o-pa and has its N-terminus acylated with the 4-pentynoic acid and its C-terminal lysine acylated with the chloroalkane tag. These results indicate that addition of the lysine and relocation of the chloroalkane tag to the C-terminus result in minimal effects on overall CAPA results. Error bars show standard error from three independent experiments. CP_{50} averages and standard errors are from three independent curve fits from three independent experiments.

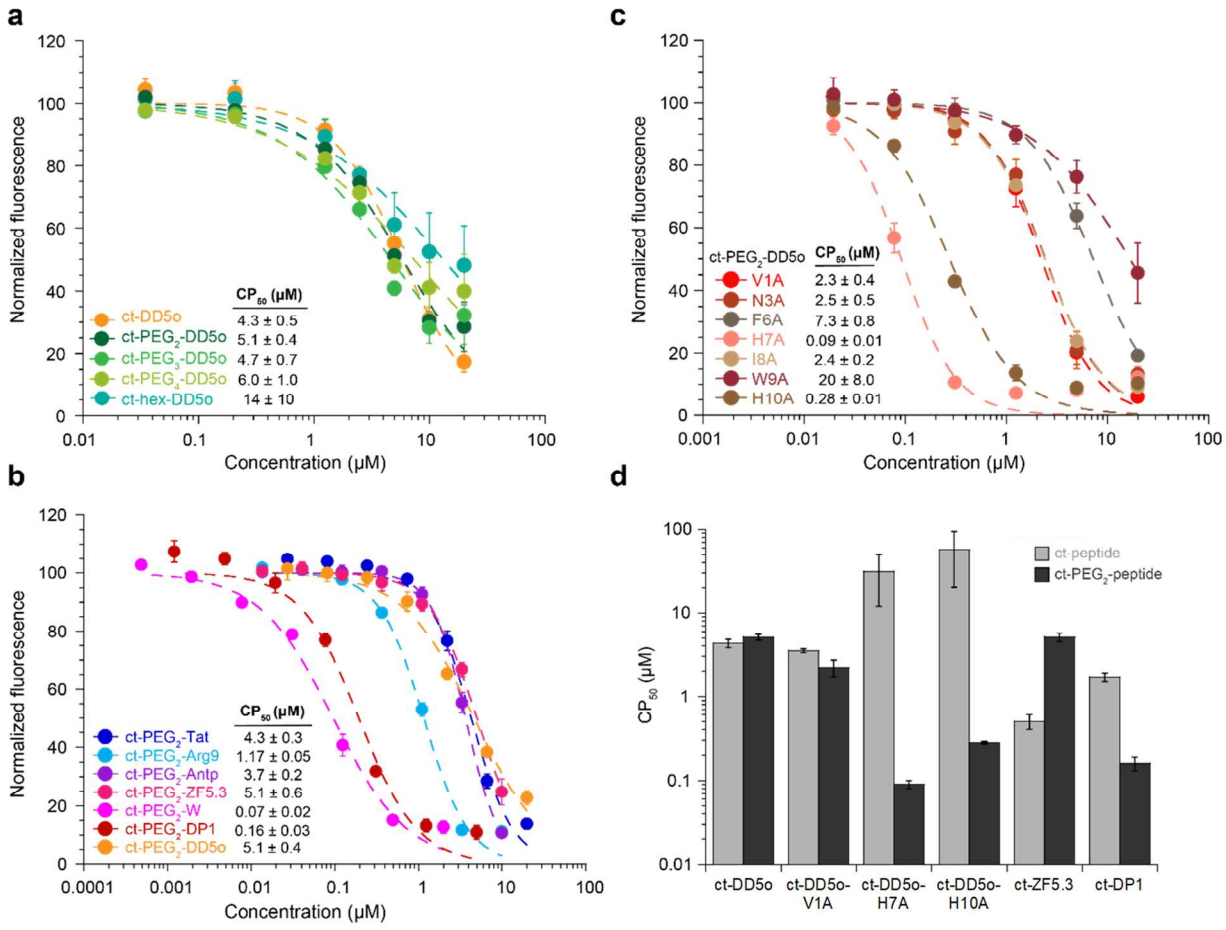

SI Figure 3. Varying linker type and length has very little effect on CAPA results for DD5o. **a.** Dose-dependent CAPA results for ct-DD5o with various linkers (see Figure S1 for linker structures). Linker structure had minimal effect on overall results, except for ct-hex-DD5o. **b.** Dose-dependent CAPA results for ct-PEG_2-Tat, ct-PEG_2-Arg9, ct-PEG_2-Antp, ct-PEG_2-ZF5.3, ct-PEG_2-W, ct-PEG_2-DP1, and ct-PEG_2-DD5o. The CP_{50} values for most ct-peptide and ct-PEG_2-peptide pairs match, meaning the linker does not have an affect CAPA data, though not for all. Most notably, ct-PEG_2-DP1 has a 10-fold lower CP_{50} over ct-DP1 (Fig.1), while ct-PEG_2-ZF5.3 has a 10-fold higher CP_{50} over ct-ZF5.3 (Fig. 1). **c.** Dose-dependent CAPA results for ct-PEG_2-DD5o alanine scan peptides. Error bars show standard error from three independent experiments. CP_{50} averages and standard errors are from three independent curve fits from three independent experiments. **d.** CAPA results for select ct-peptide and ct-PEG_2-peptide pairs. Graph shows CP_{50} values on a log scale, and error bars show standard error from three independent experiments.

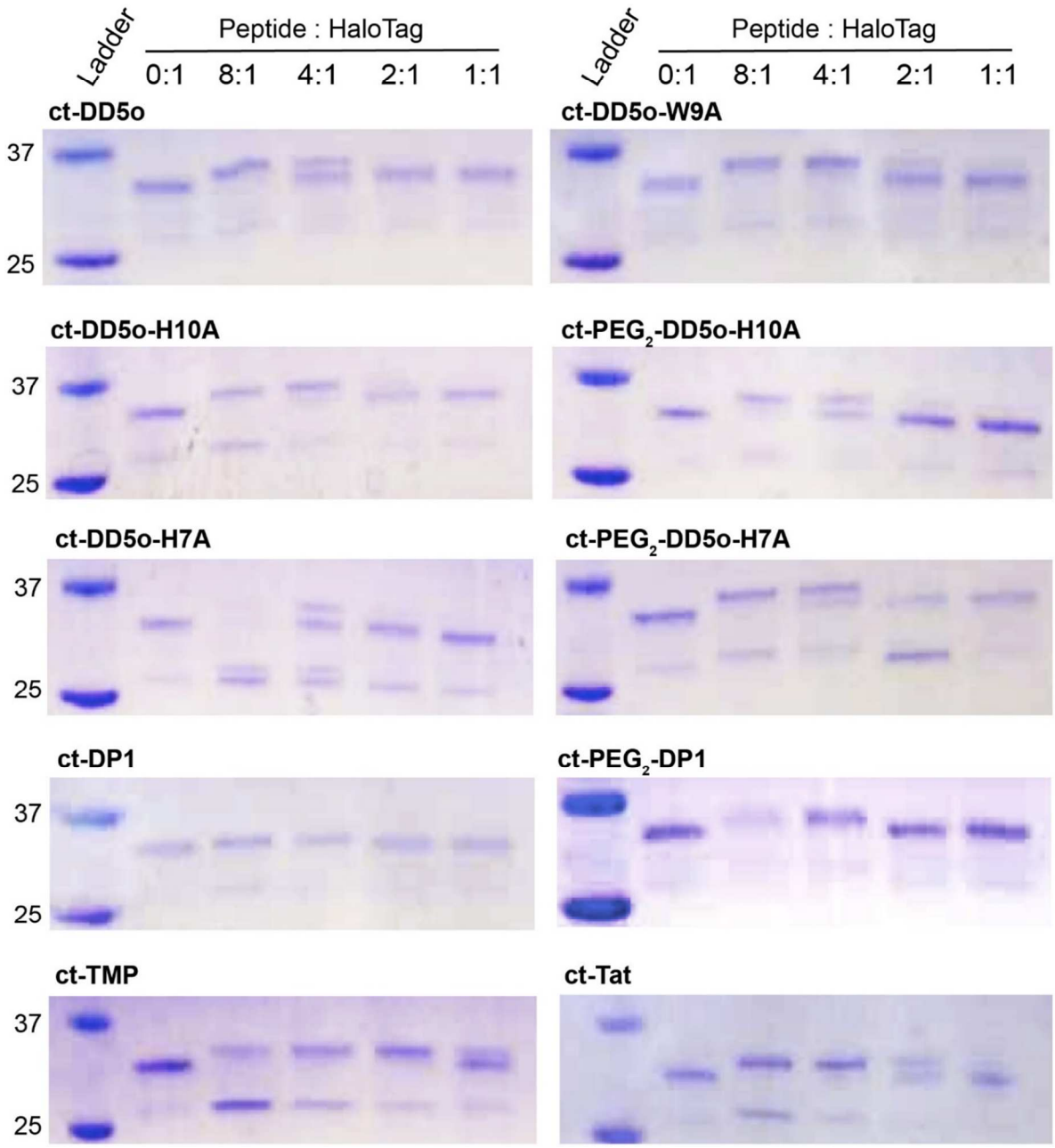

SI Figure 4. Gel-shift assay directly demonstrates extent of reaction with recombinant HaloTag *in vitro*. Recombinant purified HaloTag (5 μM) was incubated for 4h at 37°C with increasing equivalents of the indicated ct-molecule, then separated on 10% SDS-PAGE gels and stained. Band for HaloTag alone is present at 34 kDa. A distinct shift could be observed when the protein was alkylated with ct-molecule. For nearly all molecules, a ratio of 2:1 or 4:1 of ct-molecule:HaloTag was sufficient to observe an upper band, with full conversion to alkylated HaloTag consistently observed at 4:1 or 8:1 ratio. A lower MW band can be observed at roughly 28 kDa. This is a degradation product of HaloTag which we observed, to differing extents, only upon alkylation and only with recombinant HaloTag. Further work is being conducted to understand this degradation. ct-TMP is an chloroalkane-trimethoprim, previously tested with the HaloTag system.[1]

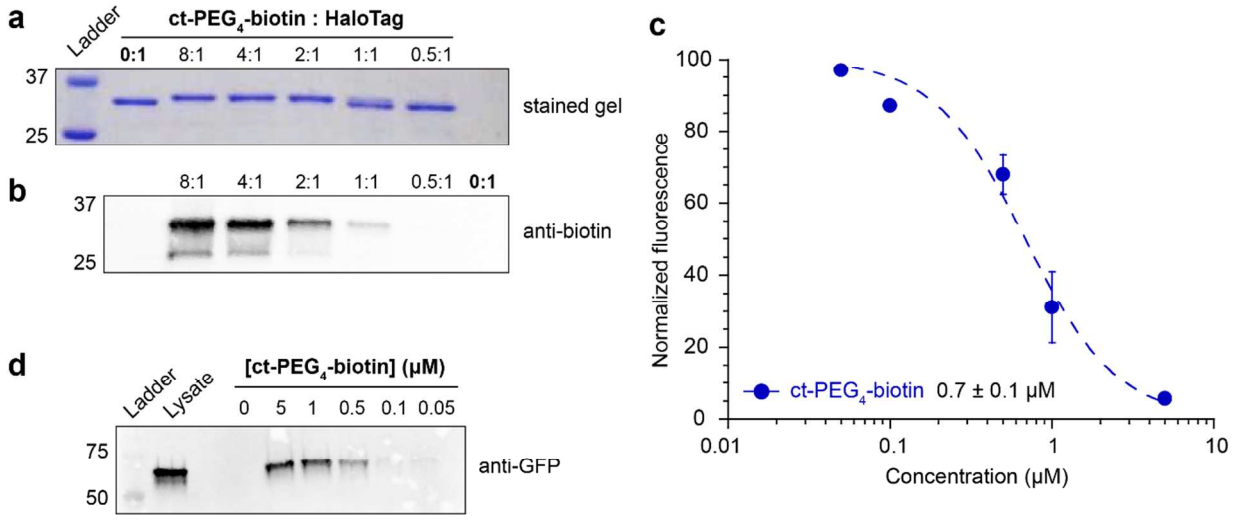

SI Figure 5. Demonstrating direct conjugation to HaloTag in cells. a. Gel-shift assay (SI Figure 4) for ct-PEG_4-biotin with recombinant HaloTag. **b.** Western blot of the reaction between ct-PEG_4-biotin and purified HaloTag, detected using anti-biotin primary Ab. **c.** Dose-dependent CAPA results for ct-PEG_4-biotin. Error bars show standard error from two independent experiments. CP_{50} averages and standard errors are from two independent curve fits from two independent experiments. **d.** Pull-down assay using lysate from Halo-GFP-Mito cell line, which were incubated with increasing concentrations of ct-PEG_4-biotin. These lysates were the same cells that were treated with ct-TAMRA and analyzed by flow cytometry in panel c. Lysates were incubated with streptavidin-magnetic beads, then the beads were washed, eluted, and blotted for anti-GFP. These results are representative of two independent experiments. The appearance of a band in the lane corresponding to incubation of cells with 0.5 µM ct-PEG_4-biotin matches the lowest concentration at which significant reduction in red fluorescence was observed in the CAPA results.

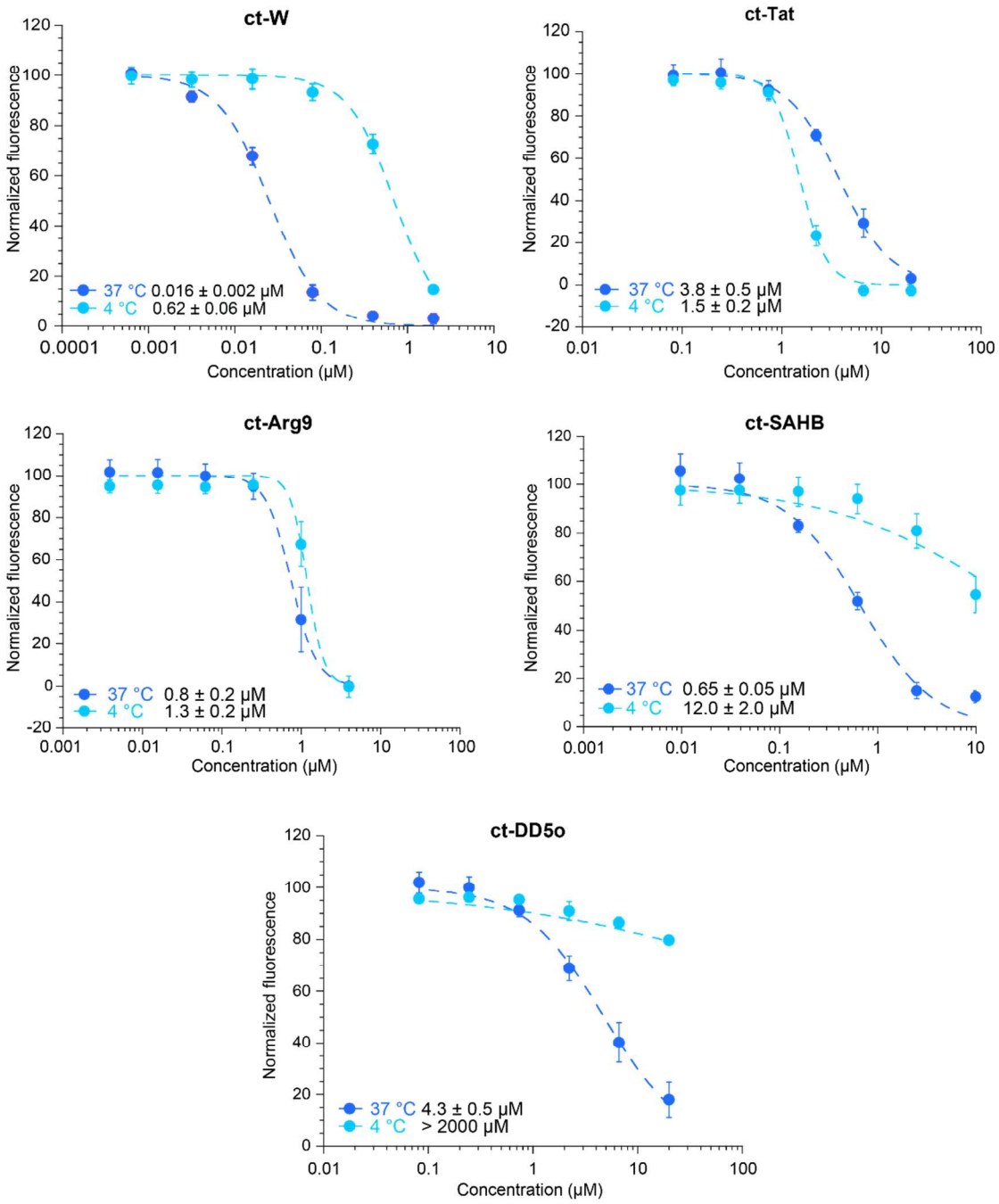

SI Figure 6. Profiling temperature dependence of cell penetration. Dose-dependent CAPA results for ct-W, ct-Tat, ct-Arg9, ct-SAHB, and ct-DD5o, tested at 37°C and 4°C. ct-molecules were incubated with cells for 4h in Opti-MEM. Error bars show standard error from three independent experiments. CP_{50} averages and standard error, shown in Fig. 2a, are from three independent curve fits from three independent experiments.

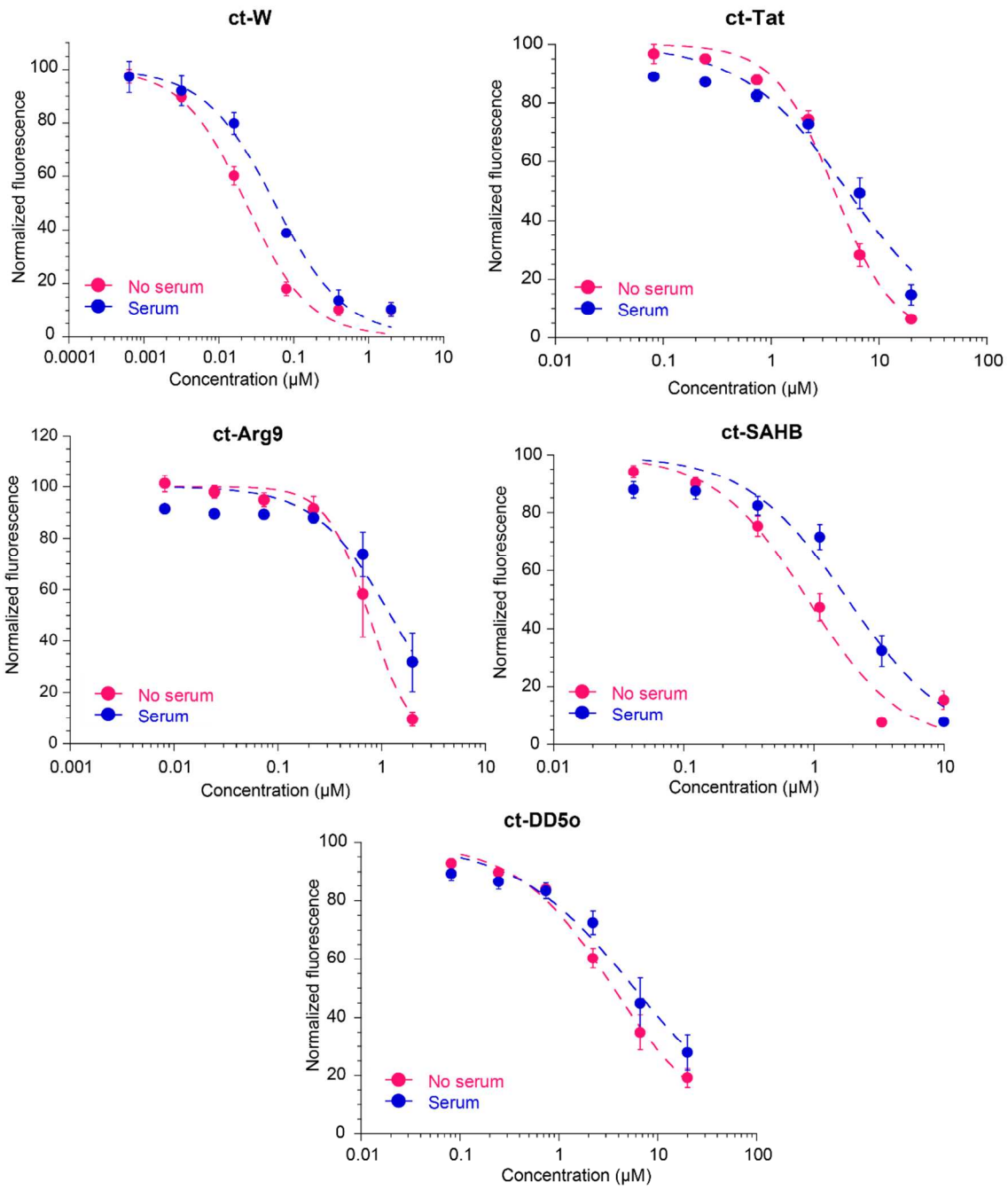

SI Figure 7. Profiling serum dependence of cell penetration. Dose-dependent CAPA results for ct-W, ct-Tat, ct-Arg9, ct-SAHB, and ct-DD5o, tested at 4h in DMEM with or without 10% FBS. Error bars show standard error from three independent experiments. CP_{50} averages and standard error, reported in Fig. 2b, are from three independent curve fits from three independent experiments.

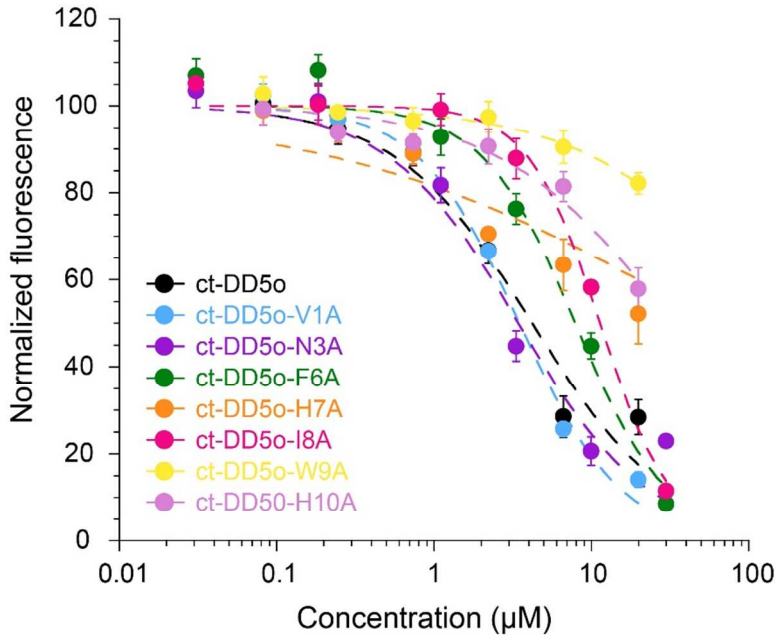

SI Figure 8. Full dose-response curves for alanine scan variants of ct-DD5o. Dose-dependent CAPA results for ct-DD5o and alanine scan variants. Cells were incubated with ct-molecules for 4h in Opti-MEM. Error bars show standard error from three independent experiments. CP_{50} averages and standard error, reported in Fig. 4a, are from three independent curve fits from three independent experiments.

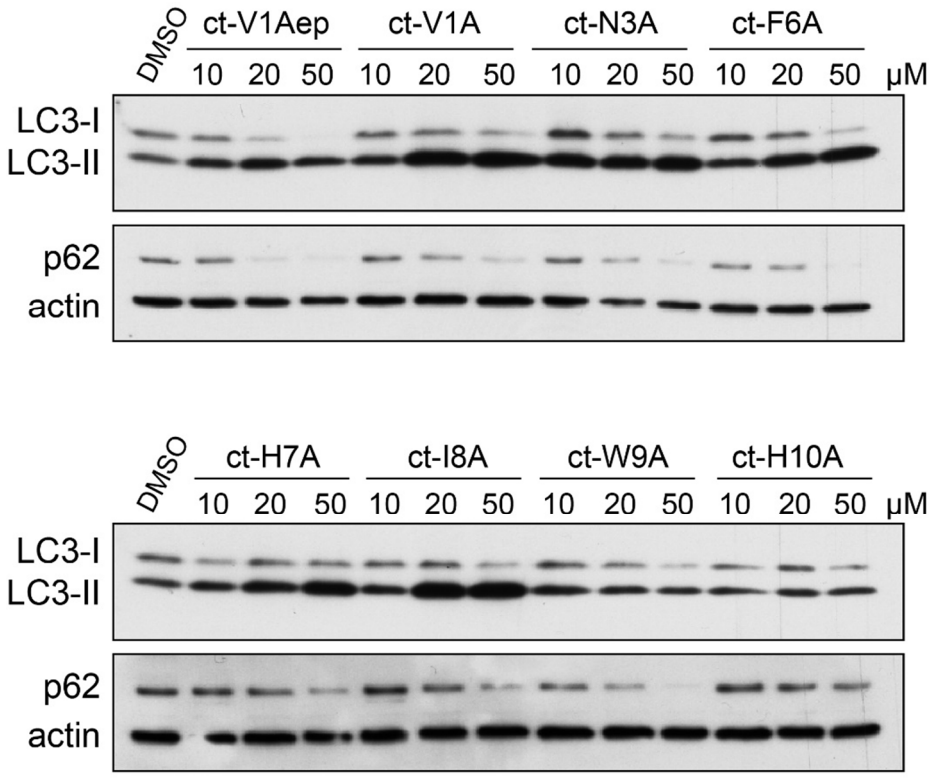

SI Figure 9. Cell-based autophagy assay for alanine scan variants of ct-DD5o. Autophagy induction was measured in HeLa cells using LC3 turnover and p62 degradation assays, using common conventions of the autophagy field.[4] Cells were treated with peptide at concentrations shown for 2h, then p62 degradation and LC3 lipidation (conversion of LC3-I to LC3-II) were analyzed by immunoblot as described.[2,3] Autophagy induction was only inferred if both p62 was degraded, and there was net conversion of LC3-I to LC3-II. Actin blots were included as internal controls.

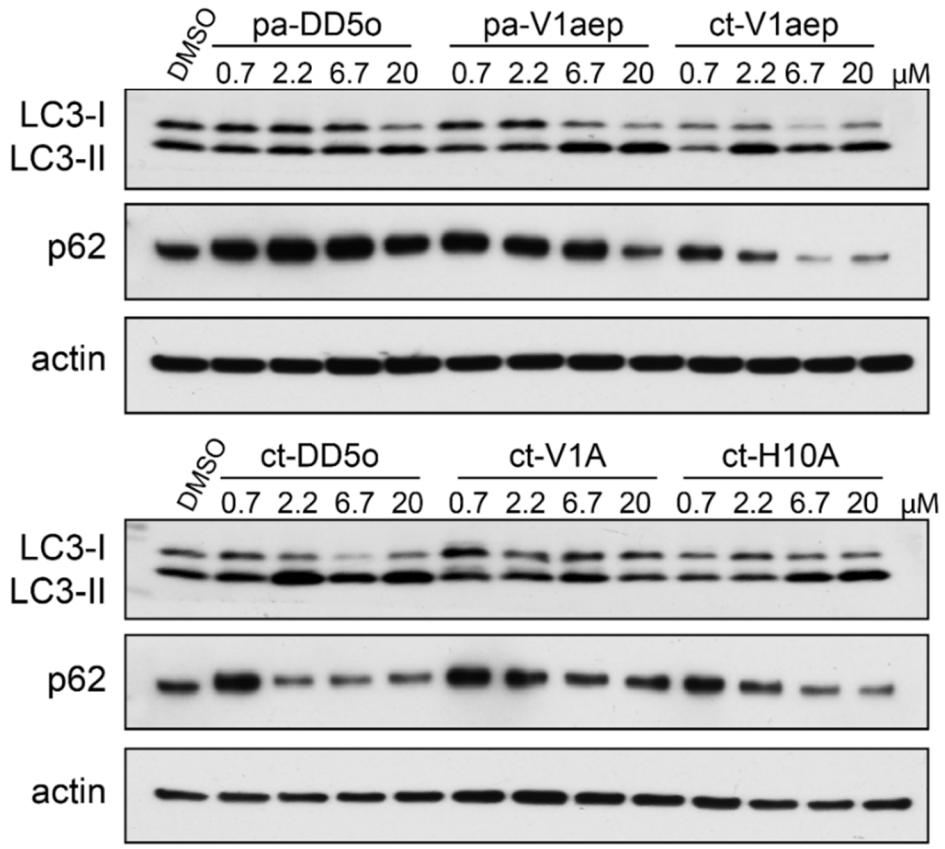

SI Figure 10. Cell-based autophagy assays for ct-DD5o and ct-V1Aep. Autophagy induction was measured in HeLa cells using LC3 turnover and p62 degradation assays, using common conventions of the autophagy field.[4] Cells were treated with peptide at concentrations shown for 2h, then p62 degradation and LC3 lipidation (conversion of LC3-I to LC3-II) were analyzed by immunoblot as described.[2,3] Autophagy induction was only inferred if both p62 was degraded, and there was net conversion of LC3-I to LC3-II. Actin blots were included as internal controls.

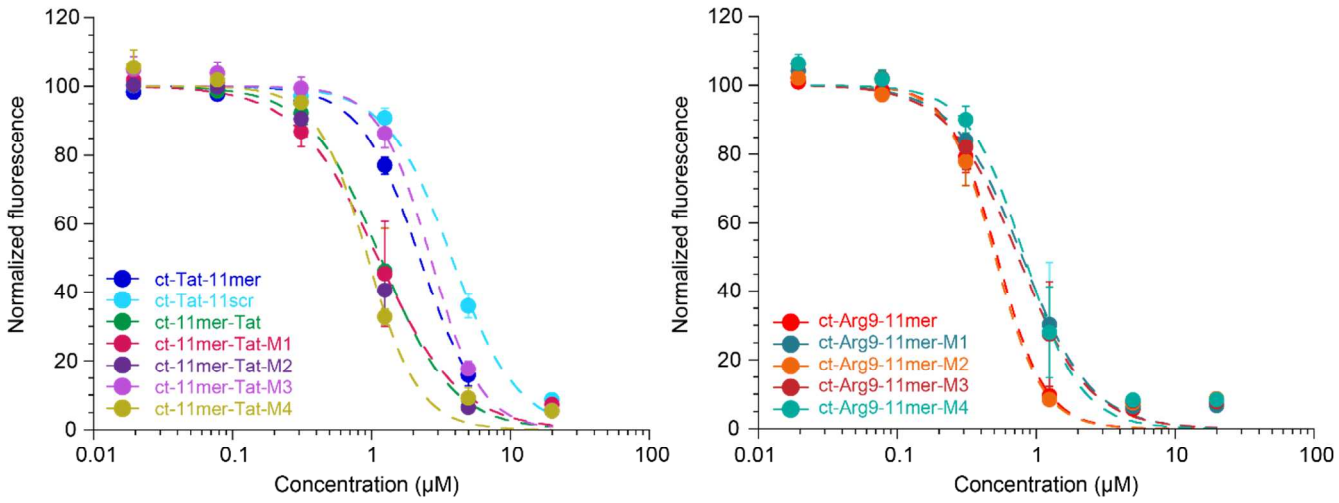

SI Figure 11. Full dose-response curves for variants of CPP-conjugated autophagy inducers. Dose-dependent CAPA results for ct-Tat-11mer and scrambled control, as well as a C-terminal Tat series, and N-terminal Arg9 series with the 11mer sequence. Cells were incubated with ct-molecules for 4h in Opti-MEM. Error bars show standard error from three independent experiments. CP_{50} averages and standard error, reported in Fig. 4d, are from three independent curve fits from three independent experiments.

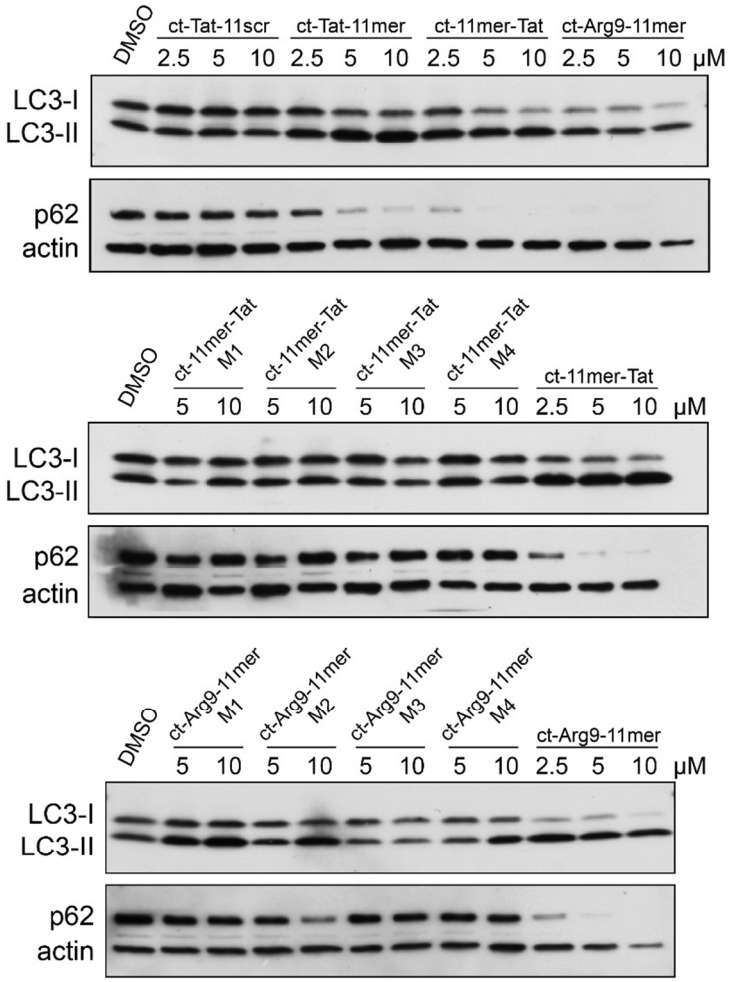

SI Figure 12. Cell-based autophagy assays for CPP-conjugated peptides. Autophagy induction was measured in HeLa cells using LC3 turnover and p62 degradation assays, using common conventions of the autophagy field.[4] Cells were treated with peptide at concentrations shown for 2h, then p62 degradation and LC3 lipidation (conversion of LC3-I to LC3-II) were analyzed by immunoblot as described.[2,3] Autophagy induction was only inferred if both p62 was degraded, and there was net conversion of LC3-I to LC3-II. Actin blots were included as internal controls.

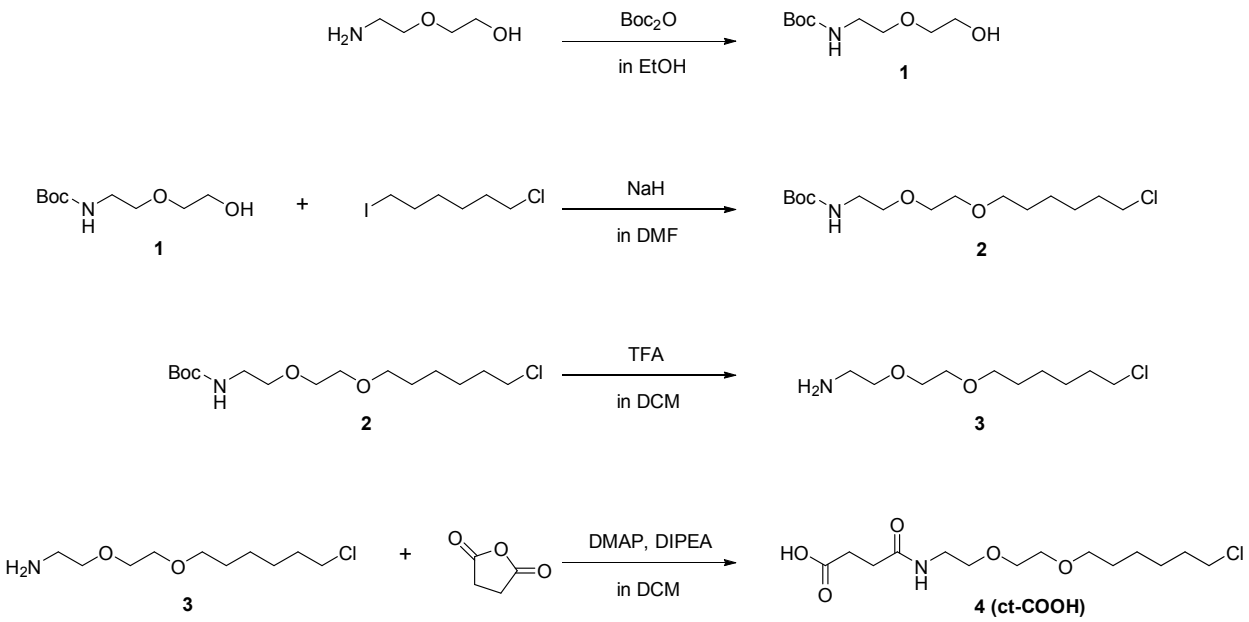

SI Figure 13. Synthesis scheme for chloroalkane carboxylate. The chloroalkane carboxylic acid was synthesized as previously described, with some modifications.[5,6] See Supporting Methods for details.

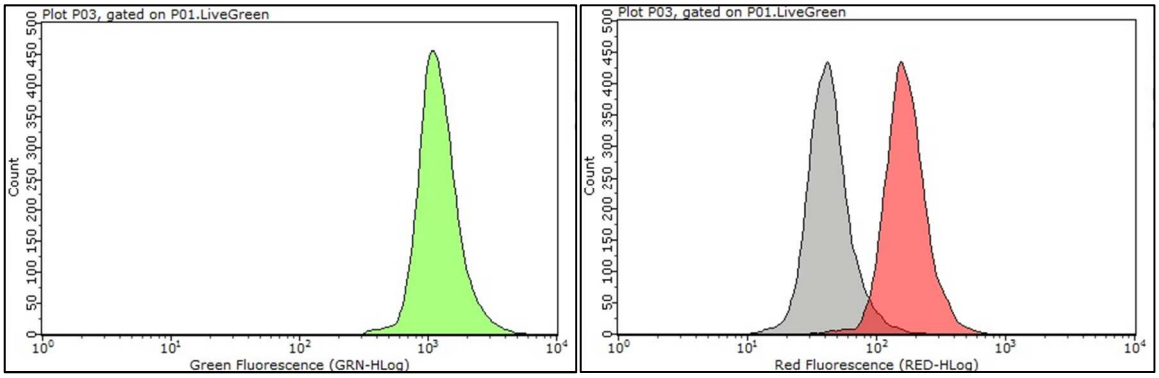

SI Figure 14. Distribution of HaloTag-GFP expression. The relatively narrow distribution of expression levels of the HaloTag-GFP-mito fusion construct can be observed in the distribution of green fluorescence (green histogram, reporting on GFP) and in the distribution of red fluorescence (red histogram, reporting on TAMRA fluorescence after cells were treated with 5 μM ct-TAMRA and washed). The gray histogram shows background red fluorescence of cells not treated with ct-TAMRA, for comparison. For these and all CAPA experiments, cells were gated for live cells with above-background intensity in the green channel, and each curve is a histogram of 10,000 cells.

SI Table 2. Temperature effects on CP_{50} values of ct-molecules
Standard error is from three independent replicates. Values correspond to data and curve fits shown in main text Figure 2a.

Molecule	CP_{50} (μM)	
	37 ºC	4 ºC
ct-W	0.016 ± 0.002	0.62 ± 0.06
ct-BIM-$SAHB_{A1}$	0.65 ± 0.05	12 ± 3
ct-DD5o	5 ± 1	2800 ± 1500
ct-Tat	3.8 ± 0.5	1.6 ± 0.2
ct-R9W	0.8 ± 0.2	1.3 ± 0.2

SI Table 3. Serum effects on CP_{50} values of ct-molecules
Standard error is from three independent replicates. Values correspond to data and curve fits shown in main text Figure 2b.

Molecule	CP_{50} (μM)	
	No serum	Serum
ct-W	0.024 ± 0.003	0.06 ± 0.01
ct-BIM-$SAHB_{A1}$	0.9 ± 0.1	1.9 ± 0.4
ct-DD5o	3.9 ± 0.7	8.5 ± 3.3
ct-Tat	3.9 ± 0.4	5.4 ± 0.9
ct-R9W	0.8 ± 0.2	1.6 ± 0.5

SI Table 4. CP_{50} values from time course experiments
Standard error is from three independent replicates. Values correspond to data and curve fits shown in main text Figure 3.

Molecule	CP_{50} (μM)				
	0.5 h	2 h	4 h	8 h	24 h
ct-W	0.25 ± 0.03	0.045 ± 0.006	0.015 ± 0.001	0.0084 ± 0.0004	0.0051 ± 0.0006
ct-Tat	600 ± 400	8 ± 1	5.6 ± 0.5	3.2 ± 0.2	1.39 ± 0.05
ct-Arg9	5 ± 2	0.62 ± 0.06	0.49 ± 0.08	0.31 ± 0.04	0.120 ± 0.009
ct-$SAHB_{A1}$	80 ± 40	1.8 ± 0.2	0.53 ± 0.08	0.29 ± 0.02	0.14 ± 0.02
ct-DD5o	1300 ± 1000	9 ± 2	3.8 ± 0.6	2.0 ± 0.2	1.00 ± 0.09

SI Table 5. CP_{50} values from alanine scan of ct-DD5o using two different ct-linkers
Standard error is from three independent replicates. Values for ct-peptides correspond to data and curve fits shown in main text Figure 4a.

Peptide	CP_{50} (μM)	
	ct-peptide	ct-PEG2-peptide
ct-DD5o	4.2 ± 0.4	5 ± 1
ct-DD5o-V1A	3.5 ± 0.2	2.2 ± 0.5
ct-DD5o-N3A	3.5 ± 0.9	2.5 ± 0.8
ct-DD5o-F6A	8 ± 2	7 ± 1
ct-DD5o-H7A	30 ± 20	0.09 ± 0.01
ct-DD5o-I8A	11 ± 1	2.4 ± 0.4
ct-DD5o-W9A	420 ± 60	20 ± 10
ct-DD5o-H10A	60 ± 40	0.28 ± 0.01

SI Table 6. CP_{50} values for autophagy-inducing CPP-peptides
Standard error is from three independent replicates. Values correspond to data and curve fits shown in main text Figure 4d.

Peptide	CP_{50} (μM)
ct-Tat-11mer	1.8 ± 0.2
ct-Tat-11scr	3.2 ± 0.5
ct-11mer-Tat	1.1 ± 0.2
ct-11mer-Tat-M1	1.0 ± 0.4
ct-11mer-Tat-M2	0.8 ± 0.2
ct-11mer-Tat-M3	2.2 ± 0.3
ct-11mer-Tat-M4	0.4 ± 0.1
ct-Arg9-11mer	0.8 ± 0.1
ct-Arg9-11mer-M1	0.8 ± 0.4
ct-Arg9-11mer-M2	0.5 ± 0.1
ct-Arg9-11mer-M3	0.8 ± 0.3
ct-Arg9-11mer-M4	0.8 ± 0.3

SI Table 7. CP_{50} values for peptides tested in nuclear and cytosolic CAPA cell lines
Standard error is from three independent replicates. Values correspond to data and curve fits shown in main text Figures 5b and 5c.

Molecule	CP_{50} (μM)	
	Nuclear	Cytosolic
ct-W	0.019 ± 0.003	0.025 ± 0.004
ct-BIM-$SAHB_{A1}$	0.81 ± 0.08	0.65 ± 0.05
ct-DD5o	2.8 ± 0.2	4.8 ± 0.7
ct-Tat	2.8 ± 0.3	3.1 ± 0.5
ct-R9W	0.36 ± 0.03	0.3 ± 0.1

Supporting Methods

Gel-shift assay. HaloTag purified protein (5 μM) was incubated with either PBS or ct-molecule at various ratios and incubated at 37 ºC for 4 hours. Samples were resolved on a 10% SDS-PAGE gel under reducing and denaturing conditions. Gel was stained and de-stained using Pierce Power Station PowerStain cassette (Thermo Fisher).

Pulldown and western blot with CAPA lysates. Cells were seeded in a 6-well plate the day before the experiment at a density of 8 x 10^5 cells per well in culture media. Cells were incubated with different concentrations of ct-molecule as described above at 37 ºC + 5% CO_2 for 4 hours, and subsequently washed with 1 mL Opti-MEM for 15 mins. Cells were trypsinized and re-suspended in PBS. After trypsinization, cells were spun down at 1,000 rpm for 3 minutes, supernatant was removed, and cells were lysed in 200 μL of RIPA lysis buffer on ice for 30 mins. Lysates were centrifuged at 4 ºC for 60 mins at >14,000 rpm, and the supernatant was transferred to a clean tube for total protein quantification using a BCA assay. For the pulldown experiment, 50 μL Pierce streptavidin magnetic beads (Thermo Fisher) were washed x3 with 1 mL TBST, then incubated with 60 μg lysate protein for 2 hours at room temperature. Beads were washed x4 with 1 mL TBST, and then pulled down protein was eluted with 100 μL Laemmli SDS-PAGE reducing buffer and heated for 5 minutes at 100 ºC. 15 μg of each sample was separated on a 7.5% SDS-PAGE gel and transferred to a nitrocellulose membrane with Pierce Power Station PowerBlot cassette (Thermo Fisher). The membrane was blocked with 5% non-fat dry milk in TBST overnight, then transferred to an iBind Flex (Invitrogen) with 1:1000 dilution of 1º anti-GFP, rabbit (Invitrogen) and 1:1000 dilution of 2º goat anti-rabbit-HRP (Thermo Fisher), or 1º anti-biotin, goat (Thermo Fisher) and 2º rabbit anti-goat (Thermo Fisher) for 4 hours. Membrane was washed with 1X TBS 3 x 5 mins, incubated with SuperSignal West Pico chemiluminescent substrate (Thermo Fisher) and developed with a ChemiDoc MP Imaging System (BioRad).

Synthesis of chloroalkane carboxylate. Synthesis scheme shown in SI Fig. 13. To start, 2.1 g (20 mmol) of 2-(2-aminoethoxy)ethanol was dissolved in 50 mL of ethanol at 0 °C and 4.36 g (20 mmol) of Boc_2O was added to the solution. The reaction was stirred for 2h at room temperature, then diluted with CH_2Cl_2 and washed with water and brine. The organic layer was dried over $MgSO_4$ and concentrated *via* rotavap to obtain colorless oil **1**. Compound **1** (3.3 g, 16 mmol) was dissolved in anhydrous DMF and placed under Ar. 0.88 g of 60% NaH mineral oil was added at 0 °C, and after 30 min, 6.1 g (24.7 mmol) of 1-chloro-6-iodohexane was added to the reaction mixture. The reaction was left to stir overnight. The reaction was quenched using 1 M HCl, and extracted using ethyl acetate. The organic layers were combined and washed using water and brine, then dried over $MgSO_4$. The crude compound was purified by column chromatography using a gradient of 20:80 ethyl acetate/hexanes to 50:50 ethyl acetate/hexanes. The fractions were combined and concentrated to obtain a yellow oil **2**. Compound **2** was dissolved in 40 mL dry CH_2Cl_2 and 10 mL TFA was added to the solution at 0 °C, then mixed for 2h at room temperature. The solvent was removed, and the material was dissolved in MeOH and treated with K_2CO_3 until the reaction was neutralized. The mixture was filtered and concentrated, then dissolved in ethyl acetate, and washed with water and brine, then concentrated to give **3**. Approximately 1 g of **3** (4.47 mmol) was dissolved in CH_2Cl_2 and placed under Ar. *N,N*-Diisopropylethyamine (1.35 mL) and 4-dimethylaminopyridine (476 mg) were added to the reaction and stirred vigorously. Succinic anhydride (800 mg, 8.0 mmol) was added and the reaction was stirred for 2h at room temperature under Ar. Reaction was quenched with 1 M HCl, and then extracted with CH_2Cl_2.The organic layers were combined, washed with brine and water, dried over $MgSO_4$, and concentrated *via* rotavap. The final product was then purified using RP-HPLC to obtain the pure chloroalkane carboxylic acid.

Immunoblot autophagy assays. Peptide was incubated with cells in Opti-MEM media (Thermo Scientific) for 2 h. Cells were washed with PBS and lysed on ice for 1 hour in lysis buffer consisting of 20 mM HEPES, 150 mM NaCl, 1 mM EDTA, 1% Triton X-100, and Roche protease inhibitor cocktail. Lysates were pelleted by centrifugation for 10 min at 4 ºC. Supernatants were separated by SDS-PAGE and transferred to a PVDF membrane. The membrane was blocked with 5% nonfat dry milk in PBS with 0.05% Tween-20 for 1 hour at room temperature. The membrane was then incubated with primary antibody in 5% milk overnight at 4 ºC, washed with PBS with 0.05% Tween-20, and then the membrane was incubated with HRP-conjugated secondary antibody in 5% milk for 1 hour at room temperature. Membrane was washed with PBS and visualized with SuperSignal West Pico Chemiluminescent Substrate (Thermo Scientific).

References

(1) Ballister, E. R.; Aonbangkhen, C.; Mayo, A. M.; Lampson, M. A.; Chenoweth, D. M. Localized Light-Induced Protein Dimerization in Living Cells Using a Photocaged Dimerizer. *Nat. Commun.* **2014**, *5*, 1–9.

(2) Shoji-Kawata, S.; Sumpter, R.; Leveno, M.; Campbell, G. R.; Zou, Z.; Kinch, L.; Wilkins, A. D.; Sun, Q.; Pallauf, K.; MacDuff, D.; Huerta, C.; Virgin, H. W.; Helms, J. B.; Eerland, R.; Tooze, S. A.; Xavier, R.; Lenschow, D. J.; Yamamoto, A.; King, D.; Lichtarge, O.; Grishin, N. V.; Spector, S. A.; Kaloyanova, D. V.; Levine, B. Identification of a Candidate Therapeutic Autophagy-Inducing Peptide. *Nature* **2013**, *494* (7436), 201–206.

(3) Peraro, L.; Zou, Z.; Makwana, K. M.; Cummings, A. E.; Ball, H. L.; Yu, H.; Lin, Y.-S.; Levine, B.; Kritzer, J. A. Diversity-Oriented Stapling Yields Intrinsically Cell-Penetrant Inducers of Autophagy. *J. Am. Chem. Soc.* **2017**, *139*, 7792–7802.

(4) Klionsky, D. J.; Abdelmohsen, K.; Abe, A.; Abedin, M. J.; Abeliovich, H.; Arozena, A. A.; Adachi, H.; Adams, C. M.; Adams, P. D.; Adeli, K.; et al. Guidelines for the Use and Interpretation of Assays for Monitoring Autophagy (3rd Edition). *Autophagy* **2016**, *12* (1), 1–222.

(5) Vistain, L. F.; Rotz, M. W.; Rathore, R.; Preslar, A. T.; Meade, T. J. Targeted Delivery of Gold Nanoparticle Contrast Agents for Reporting Gene Detection by Magnetic Resonance Imaging. *Chem. Commun.* **2016**, *52* (1), 160–163.

(6) So, M. kyung; Yao, H.; Rao, J. HaloTag Protein-Mediated Specific Labeling of Living Cells with Quantum Dots. *Biochem. Biophys. Res. Commun.* **2008**, *374* (3), 419–423.